AFWL-TN-
84-22



# COLLISION-INDUCED DIPOLE MOMENTS

T.F. Gallagher

SRI International
333 Ravenswood Ave
Menlo Park, CA 94025

October 1984

Final Report

Approved for public release; distribution unlimited.





AIR FORCE WEAPONS LABORATORY
Air Force Systems Command
Kirtland Air Force Base, NM 87117

This final report was prepared by the SRI International, Menlo Park, California, under Contract F29601-83-K-0043, Job Order ILIR8314 with the Air Force Weapons Laboratory, Kirtland Air Force Base, New Mexico. Captain John A. Filcoff (ARDA) was the Laboratory Project Officer-in-Charge.

When Government drawings, specifications, or other data are used for any purpose other than in connection with a definitely Government-related procurement, the United States Government incurs no responsibility or any obligation whatsoever. The fact that the Government may have formulated or in any way supplied the said drawings, specifications, or other data, is not to be regarded by implication, or otherwise in any manner construed, as licensing the holder, or any other person or corporation; or conveying any rights or permission to manufacture, use, or sell any patented invention that may in any way be related thereto.

This report has been authored by a contractor of the United States Government. Accordingly, the United States Government retains a nonexclusive, royalty-free license to publish or reproduce the material contained herein, or allow others to do so, for the United States Government purposes.

This report has been reviewed by the Public Affairs Office and is releasable to the National Technical Information Services (NTIS). At NTIS, it will be available to the general public, including foreign nations.

If your address has changed, if you wish to be removed from our mailing list, or if your organization no longer employs the addressee, please notify AFWL/ARDA, Kirtland AFB, NM 87117 to help us maintain a current mailing list.

This technical report has been reviewed and is approved for publication.

JOHN A FILCOFF
Captain, USAF
Project Officer

FOR THE COMMANDER

GERALD A. HASEN
Major, USAF
Chief, Oxygen-Iodine Laser Branch

WILLIAM M. BROWNING
Lt Colonel, USAF
Chief, Laser Device Division

---

DO NOT RETURN COPIES OF THIS REPORT UNLESS CONTRACTUAL OBLIGATIONS OR NOTICE ON A SPECIFIC DOCUMENT REQUIRES THAT IT BE RETURNED.

UNCLASSIFIED
SECURITY CLASSIFICATION OF THIS PAGE

AD-A147682

## REPORT DOCUMENTATION PAGE

| | |
|---|---|
| 1a. REPORT SECURITY CLASSIFICATION<br>Unclassified | 1b. RESTRICTIVE MARKINGS |
| 2a. SECURITY CLASSIFICATION AUTHORITY | 3. DISTRIBUTION/AVAILABILITY OF REPORT<br>Approved for public release; distribution unlimited. |
| 2b. DECLASSIFICATION/DOWNGRADING SCHEDULE | |
| 4. PERFORMING ORGANIZATION REPORT NUMBER(S) | 5. MONITORING ORGANIZATION REPORT NUMBER(S)<br>AFWL-TN-84-22 |
| 6a. NAME OF PERFORMING ORGANIZATION<br>SRI International | 6b. OFFICE SYMBOL (If applicable) |
| | 7a. NAME OF MONITORING ORGANIZATION<br>Air Force Weapons Laboratory |
| 6c. ADDRESS (City, State and ZIP Code)<br>333 Ravenswood Ave<br>Menlo Park, CA 94025 | 7b. ADDRESS (City, State and ZIP Code)<br>Kirtland Air Force Base, NM 87117 |
| 8a. NAME OF FUNDING/SPONSORING ORGANIZATION | 8b. OFFICE SYMBOL (If applicable) |
| | 9. PROCUREMENT INSTRUMENT IDENTIFICATION NUMBER<br>F29601-83-K-0043 |
| 8c. ADDRESS (City, State and ZIP Code) | 10. SOURCE OF FUNDING NOS. |

| PROGRAM ELEMENT NO. | PROJECT NO. | TASK NO. | WORK UNIT NO. |
|---|---|---|---|
| 61101F | ILIR | 83 | 14 |

11. TITLE (Include Security Classification)
COLLISION-INDUCED DIPOLE MOMENTS (U)

12. PERSONAL AUTHOR(S)
Gallagher, T. F.

| 13a. TYPE OF REPORT | 13b. TIME COVERED | 14. DATE OF REPORT (Yr., Mo., Day) | 15. PAGE COUNT |
|---|---|---|---|
| Final Report | FROM Jun 83 TO Dec 83 | 1984 October | 38 |

16. SUPPLEMENTARY NOTATION
Sub 1/2 Sub 5/2 Sub 3/2 Sub 7/2 n is greater than or =

| 17. COSATI CODES | | |
|---|---|---|
| FIELD | GROUP | SUB. GR. |
| 20 | 05 | |

18. SUBJECT TERMS (Continue on reverse if necessary and identify by block number)
High Energy Laser (HEL), Chemical Laser, Metastable State, Forbidden Transition, Collision Induced Gain, Line Broadening Theory

19. ABSTRACT (Continue on reverse if necessary and identify by block number)

Experimental studies of collision induced absorption of forbidden transitions have been conducted on Cs($6s_{1/2}$ - $5d_{5/2}$), Na($nd_{3/2}$ - $nf_{5/2}$) and Na($nd_{3/2}$ - $ng_{7/2}$), $n \geq 15$. Perturbers utilized include heavy rare gases, molecular dipoles, and positive ions. A very strong enhancement of the forbidden Rydgerg transitions in Na was observed and attributed to ionic space charge.

| 20. DISTRIBUTION/AVAILABILITY OF ABSTRACT | 21. ABSTRACT SECURITY CLASSIFICATION |
|---|---|
| UNCLASSIFIED/UNLIMITED ☐ SAME AS RPT. ☐ DTIC USERS ☒ | Unclassified |

| 22a. NAME OF RESPONSIBLE INDIVIDUAL | 22b. TELEPHONE NUMBER (Include Area Code) | 22c. OFFICE SYMBOL |
|---|---|---|
| Capt Gobel | (505) 844-8212 | ARDA |

DD FORM 1473, 83 APR EDITION OF 1 JAN 73 IS OBSOLETE.

UNCLASSIFIED
SECURITY CLASSIFICATION OF THIS PAGE

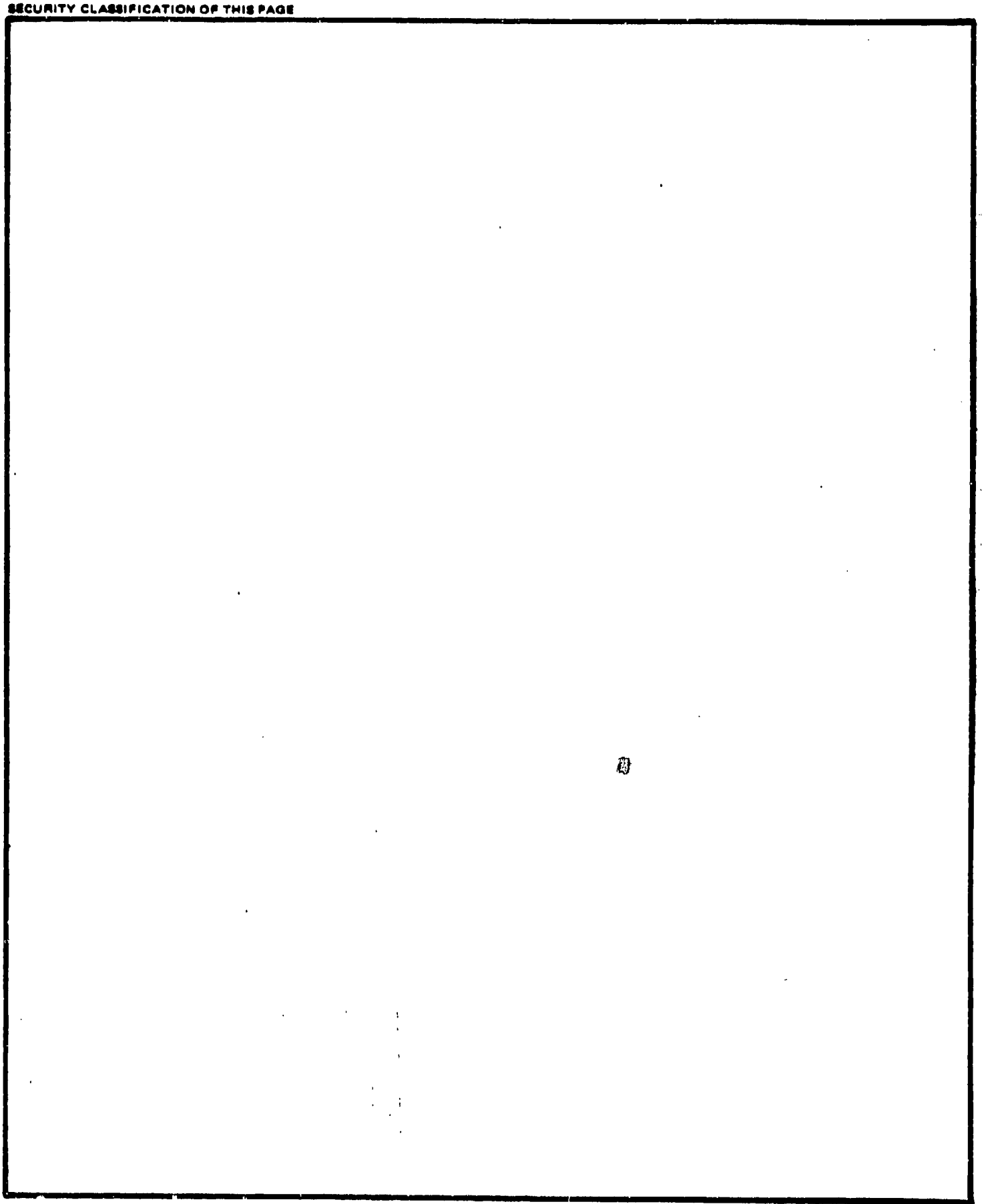

## I. Introduction

Collision-induced electric dipole moments have been proposed as a method of increasing the gain of atomic transitions other than electric dipole transitions, such as magnetic dipole and electric quadrupole transitions.[1] An example of this is the atomic I — a transition that can be photolytically produced primarily in the $P_{1/2}$ state, which is 7000 $cm^{-1}$ above the ground $P_{3/2}$ state. Because this is a magnetic dipole transition, it is necessarily much weaker, ~ $10^{-6}$, than an electric dipole transition. The gain of a laser based on such a system is necessarily low, although large amounts of energy can be stored conveniently.

The mechanism by which the collisions induce the electric dipole moment is to admix a small amount of wave function of an opposite parity atomic state. This can be done at short range by using virtually any atom or molecule, which then forms a transient molecule. An example of this is Cs-Ar or CsXe, that develops an electric dipole transition on the molecular curves that corresponds asymptotically to the Cs 6s-5d transition.[2,3] Unfortunately, the dipole moment occurs over a broad spectral range, reflecting the varying internuclear separations of the Cs and Xe atoms, and there is therefore no appreciable increase in gain.

If, on the other hand, ions or perhaps even molecules with permanent dipole moments are used, the long range electrostatic interaction between the ion or dipole and the Cs atom may be used to admix atomic Cs states of opposite parity; thus, for example, the Cs 6s-5d transition may be given an electric dipole moment.[1] Because of the longer range of the interaction, it is not unreasonable to hope for less broadening of the induced transition.

In this report we describe experiments to probe the gain induced by collisions with ions and polar molecules. Specifically we have observed that the presence of ions, by virtue of their space charge, does induce dipole moments in Rydberg atoms and allow the observation of $\Delta\ell = 2$ transitions. We found, though, that the polar molecule CO does not enhance the Cs 6s-5d quadrupole transition.

## II. Rydberg Atoms and Ions

A full report of our activity using thermal ions is included as an appendix; hence, only a brief summary of this work is given below.

Using thermal ions we have shown that we are able to induce a dipole moment in the Na nd-ng microwave transitions using very low concentrations of ions, $10^6 cm^{-3}$, because of the macroscopic space charge of the ions. The induced dipole moments, ~ 1 $ea_0$, are ~ 1% of the nd-nf dipole moments and are in agreement with theoretical estimates. Unfortunately, a substantial amount of broadening accompanies the induced dipole moment, and we suspect that this will generally be true when dipole moments are induced in nominally quadrupole transitions.

## III. Collisional effects on the Cs 6s-5d Quadrupole Transition

As a prototype system we chose to study the Cs 6s-5d quadrupole transition. The relevant energy levels of Cs are shown in Figure 1. From Figure 1 it is apparent that a dipole moment is created in the Cs 6s-5d transition by admixing some of the nearby 6p state into the 5d state so that the d state becomes[4]

$$|d\rangle = |d\rangle + \varepsilon|p\rangle \qquad (1)$$

where

$$\varepsilon = \langle p|\mu|d\rangle \, E/\Delta W \qquad (2)$$

Here $|d\rangle$ and $|p\rangle$ are the 5d and 6p states. E is the electric field, $\mu$ is the atomic dipole operator, and $\Delta W$ is the energy separation between the 6p and 5d states. The oscillator strength from the ground state to the 6p state, $f_{6s-6p}$ ~ 1,[5] and the oscillator strength to the 5d state $f_{6s-5d}$ is reduced by $(r/\lambda)^2$ where r is the radius of the atom and $\lambda$ is the wavelength of the light. For our case then, $f_{6s-5d} \sim 10^{-6}$. To make the dipole-induced oscillator strength of the 6s-5d transition equal to the strength of the quadrupole transition, for example, requires that $\varepsilon \sim 10^{-3}$. Taking the order of magnitude values (in atomic units) $\langle p|\mu|d\rangle = 10$ and $W = 10^{-2}$, we find that for $\varepsilon = 10^{-3}$, it is necessary that $E = 10^{-4}$. For CO, with a dipole moment of 0.1 $d^6$, this occurs at ~ 10 Å. For pressures in the 10-100 torr range, we can expect to have some reasonable probability of CO molecules being within 10 Å of a Cs

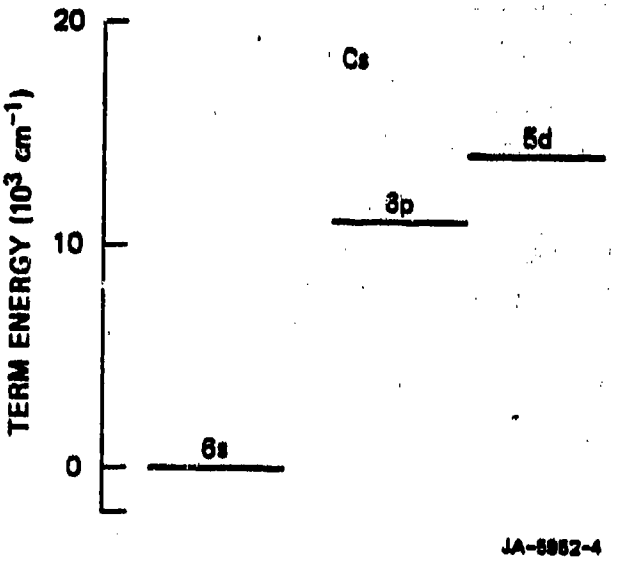


FIGURE 1 Cesium term energy diagram

atom. Unfortunately, 10 Å corresponds to a collision cross section of 100 $Å^2$, which is a good estimate of the quenching cross section.[7]

Our method of approach is to use a tunable dye laser to excite Cs atoms from the 6s state to the vicinity of the 5d state. Atoms excited to the 5d state are then photoionized, and the ions are collected. The apparatus used for this work is shown in Figure 2. It includes a Nd:YAG laser beam that is doubled to 5320 Å and split in half. One-half of the beam is used to pump the dye laser operating at ~ 6800 Å. The second half of the 5320 Å beam is then optically delayed and both beams are passed through the Cs cell. The cell is a Pyrex cylinder, 10 cm long and 4 cm in diameter, which is contained in an oven heated to 75°C to produce a Cs pressure of ~ $10^{-4}$ torr.[8] The cell has two internal electrodes 1 cm apart. One is connected to a positive voltage that is varied from 1V to 60V. The second electrode is connected to an amplifier of 10 k Ω input impedance. The ion signals appear as 3-μs-long pulses, which are measured with a gated integrator and recorded.

This arrangement is usable, but it has one flaw: The windows tend to build up Cs oxides that scatter the laser light onto the Cs-coated electrodes producing photoelectrons. Thus, after the cell is filled with Cs, the running time is limited to two days. Differentially heated windows and more sophisticated electrode design would substantially alleviate this problem.

With this apparatus we have been able to observe the Cs 6s-5d quadrupole transition, f ~ $10^{-6}$, quite easily. Figure 3 shows a recording of the ion signal as the dye laser is scanned across the $6s_{1/2}$-$5d_{5/2}$ transition. As expected, the magnitude of this signal does not depend on the applied voltage. As shown in Figure 3a, there is a small background signal due to the scattered laser light ejecting photoelectrons from Cs-coated electrodes.

When molecular gases were added, we observed in all cases a diminution of the signals. Figure 3b shows the Cs 6s-5d signal with 16 torr of CO added. The signal is clearly diminished by the addition of CO. In fact, this is generally true for all the molecular gases we used. These gases and the pressures used are summarized in Table I.

In contrast to molecular gases, atomic gases Ar and Xe did not have an obvious effect on the signal at pressures of up to 100 torr. At 500 torr of Xe, however, we observed the Cs-Xe collision-induced, or molecular, absorp

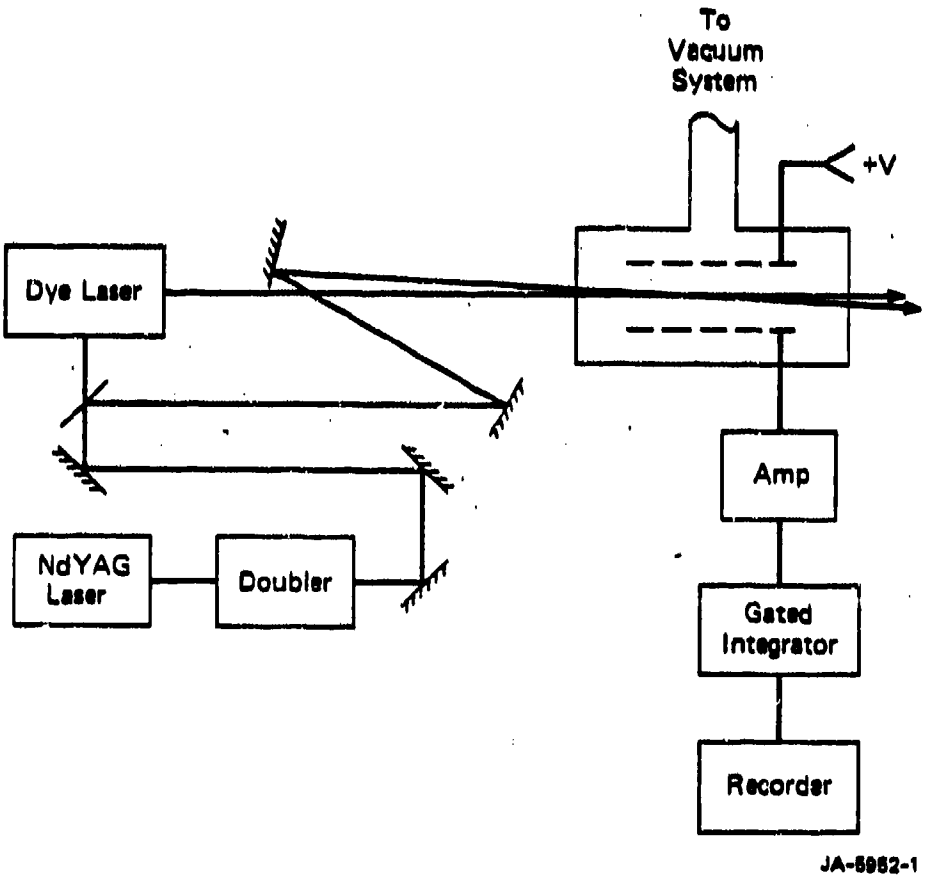


FIGURE 2 Diagram of the apparatus showing the Nd:YAG laser, dye laser, Cs cell, and detection electronics.

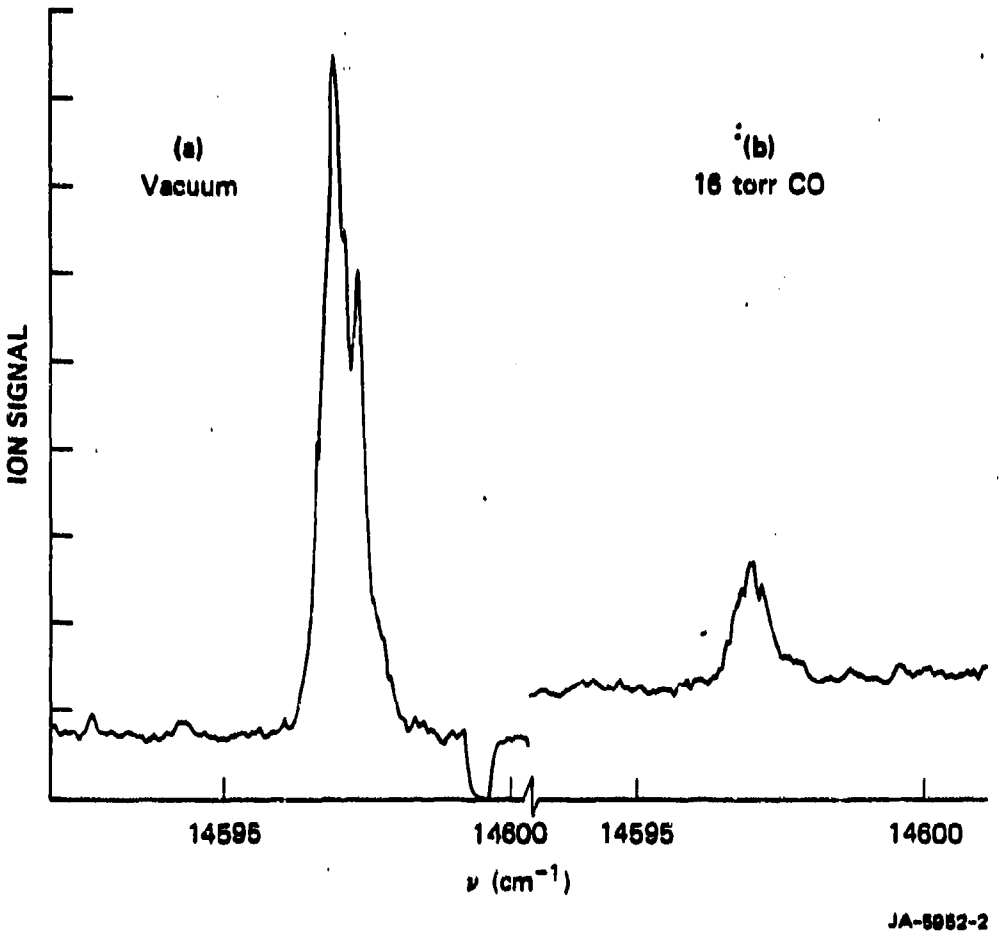


FIGURE 3 Ion signals obtained at the Cs 6s-5d quadrupole transition with (a) no gas, (b) 16 torr of CO. The CO quite evidently diminishes the signal.

Table I Perturbing Gases and Pressures

| Gas | Maximum pressure (torr) |
|---|---|
| Ar | 47 |
| Xe | 505 |
| CO | 16 |
| $CH_4$ | 27 |
| $N_2$ | 25 |
| $H_2$ | 24 |

tions shown in Figure 4. The collision-induced absorption is very broad, covering hundreds of wavenumbers. We see no reason why molecular perturbers at such high pressures would not lead to similar broadening.

As a result of these experiments, it appears that the use of the polar molecule CO is not very promising as a means of raising the gain of laser transitions, because the addition of molecular gases in the 30-torr range usually completely destroys the quadrupole signal. If pressures on this order are not sufficient to produce enhanced gain, then much higher pressure (~ 300 torr) would be required; at this point broad structure such as that shown in Figure 4 must be anticipated and quenching of the excited atoms would proceed at a rapid rate, ~ $10^9$-$10^{10}$ $s^{-1}$, for quenching cross sections of 100 $A^2$.

We note that these experiments were performed with CO, which has a weak dipole moment, ~ 0.1 d, and there exist molecules that have dipole moments two orders of magnitude larger. However, we also note that our standard of comparison for the oscillator strength was the Cs 6s-5d quadrupole transition f ~ $10^{-6}$. Thus, even a small increase, $10^{-6}$, in oscillator strength would have been readily observable.

We conclude that increases in the oscillator strength must be < $10^{-7}$. Unfortunately, the reactivity of very polar molecular gases, such as HBr and HCl, precludes their use with Cs. Nonetheless, we can extrapolate our CO value to molecules with large dipole moments. For dipole moments of 10 d and pressures of 20 torr, which is probably an upper limit due to quenching and broadening considerations, we expect an oscillator strength increase of at most $10^{-3}$, which is not remarkable for a laser.

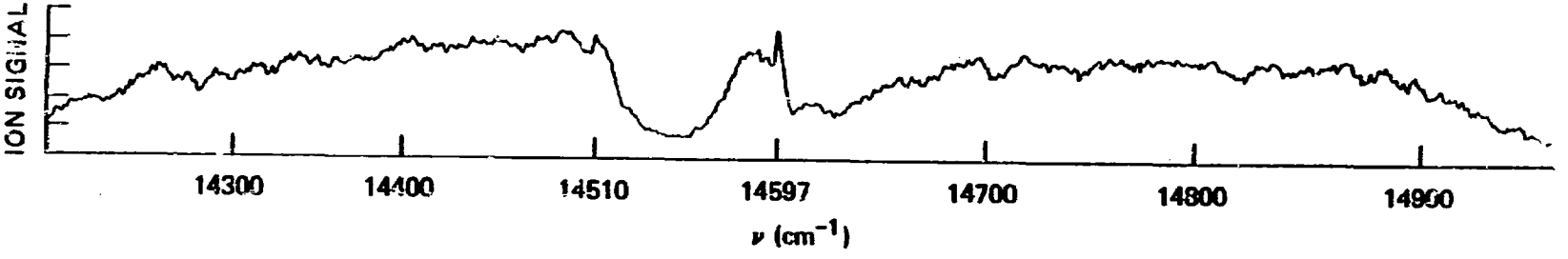


FIGURE 4 Ion signal obtained with 500 torr/Xe. This is the molecular Cs-Xe absorption.

## REFERENCES


1. D. Rogovin and P. Avizonis, Appl. Phys. Lett. 38, 666 (1981).
2. J. Pascale and J. Vandeplanque, J. Chem. Phys. 60, 2278 (1974).
3. G. Moe, A. C. Tam, and W. Happer, Phys. Rev. A 14, 349 (1976).
4. A. Messiah, Quantum Mechanics (Wiley, New York, 1958).
5. A. Lindgard and S. E. Neilsen, Data Nucl. Data Tables 19, 533 (1977).
6. K. P. Huber and G. Herzberg, Constants of Diatomic Molecules (van Nostrand, New York, 1979).
7. P. L. Lijnse, Review of Literature on Quenching, Excitation and Mixing Cross Section for the First Alkali Resonance Doublets of the Alkalis (Fysisch Laboratorium Report i 398, Utrecht, 1972).

## APPENDIX

## THE INFLUENCE OF THERMAL IONS ON THE $nd_{3/2}$-$nf_{5/2}$ AND $nd_{3/2}$-$ng_{7/2}$ MICROWAVE TRANSITION OF SODIUM

# THE INFLUENCE OF THERMAL IONS ON THE $nd_{3/2}$-$nf_{5/2}$ AND $nd_{3/2}$-$ng_{7/2}$ MICROWAVE TRANSITION OF SODIUM

H. B. van Linden van den Heuvell, N. H. Tran,
R. Kachru and T. F. Gallagher
Molecular Physics Department
SRI International
Menlo Park, CA 94025

Abstract

We have studied the dipole-allowed $nd_{3/2}$-$f_{5/2}$ and the dipole-forbidden $nd_{3/2}$-$g_{7/2}$ transitions of sodium in the presence of thermal ions for n=15-17. Although the cross sections for the relevant ion-Rydberg atom collisions are too small to influence the observed transitions, these microwave resonance measurements indicate that there is a remarkable influence of even very low densities, $10^5$ $cm^{-3}$, ions on the atoms. For instance, the d-g transition can be easily driven with a single photon, and the d-f and d-g transitions are shifted and broadened. Furthermore, the thermal sodium ions destroy the interference fringes obtained with the Ramsey method of separated oscillatory fields. Although these results are incompatible with reasonable estimates of ion-atom collision cross sections, they may be explained quantitatively in terms of the time-averaged charge of the ions.

MP 84-048
04/12/84

## I. Introduction

Recently it has been suggested that the long range ion-atom interaction may be used to increase the transition probability of magnetic dipole or electric quadrupole transitions by admixing states of the opposite parity. Such an approach could be used, for example, to raise the gain of a weak laser transition.[1,2] For lower-lying atomic states it is evident that high ion densities are required. However, this phenomenon may apparently be studied quite easily using atomic Rydberg states, because of their large dipole moments and small energy spacings. In addition, the interaction of Rydberg atoms with ions is interesting both in its own right and from the point of view of the effects on possible applications of Rydberg atoms such as far infrared detection.

Here we describe the experimental investigation of the effect of thermal ions on the allowed nd-nf and the forbidden nd-ng transitions in Na Rydberg states using microwave resonance techniques. We find that for extremely low densities of ions, orders of magnitudes less than had been expected, we observe shifts and broadenings of the allowed nd-nf transition as well as the appearance of the nd-ng transition. We attribute the observation to the macroscopic space charge field of the ions. We first describe our experimental approach and results. We then compare the results to estimates based on the interaction of a Rydberg atom with the field of one ion and with the macroscopic space charge field to show that the latter interaction must be responsible.

## II. Experimental

Since our approach has already been described,[3] we give only a short resume of the basic features. The method used to measure the d-f and d-g intervals is illustrated by the level diagram of Figure 1. The sodium is excited from the ground state $3s_{1/2}$ to $3p_{1/2}$ and then to $nd_{3/2}$ by means of two pulsed dye lasers, which are pumped with the second and the third harmonics of a Nd:YAG laser. In general, we detect the infrared 3d-3p fluorescence at 820 nm, and it accompanies a microwave transition to either a nf or ng state using a Wrattan 78 filter and an EMI 9558 photomultiplier. There is some background fluorescence due to cascades originating from the nd state, but the increase in 820 nm fluorescence when the microwave frequency is tuned through the resonance is easily observed. The Na vapor is contained in a Pyrex cell heated to 150 C, which produces a sodium vapor pressure of $4 \times 10^{-5}$ torr. The pressure of the background gas is $<10^{-6}$ torr. A Hewlett-Packard 8690B sweep oscillator is used to drive the transitions, and the microwaves are introduced into the sodium cell by means of a microwave horn. A typical power required to drive an nd-nf transition is ~ 0.1 μw. The detected infrared fluorescence signal is integrated by a PAR 162 boxcar averager, the output of which is recorded on the y channel of an x-y recorder. On the x channel the analog output of a HP 5340A frequency counter is recorded while the frequency of the microwave source is slowly swept. The instrumental frequency resolution is determined by the 50-kHz instability of the microwave source on a time scale smaller than the integration time of the averager (typically 1 s). Frequency drifts on a longer time scale become part of the frequency scan.

The thermal ions are made by photo-ionization of the Na $3p_{1/2}$ state by means of the third harmonic of the Nd:YAG laser. The density of the ions is varied by the attenuation of the 355-nm third harmonic radiation with glass

microscope slides. The neutral density of a microscope slide at 355 nm is measured to be 0.051. The typical attenuation of the UV beam needed to produce the desired amount of ions was between 10 and 30 microscope slides. Inside one of our two cells are two stainless steel mesh plates 1 cm apart. The number of ions that are generated in each laser shot is measured by applying a 4-μs-long, 50-V pulse to one plate about 1 μs after each laser shot. The ion signal at the other plate is then amplified with a fast operational amplifier and measured with a boxcar averager. It is assumed that the drift of all electrons produced is so fast that they are no longer between the plates after 1 μs. Since the microwave field is somewhat disturbed by the presence of the metal plates, which leads to broader resonance peaks, we used cells both with and without plates. In the cell without plates, we cannot make absolute ion number measurements, but only relative measurements, which may be normalized to the measurements made using the cell with plates.

## III. Observations

### 1. Resonance peaks

The shift and the broadening of d-f and d-g transitions are measured by scanning the microwave frequency in the vicinity of the resonance frequency and recording the population of the final state for different densities of the disturbing ions. Figure 2 gives a few examples of such measurements in the case of a $16d_{3/2}$-$16f_{5/2}$ transition. By doing this kind of measurement systematically as a function of the ion density, we obtain the results shown in Figure 3. Although the data are somewhat scattered, we still can see a linear dependance between the shift and $n_i^2$, where $n_i$ is the ion density indicating that we still have a low enough ion density that the Stark shift is in the quadratic regime. A compilation of the observed shifts is given in Table 1. From the same data we can also obtain the broadening of the transition, and these results are shown in Figure 4. The broadening does not extrapolate back to zero for low ion densities because of the finite frequency resolution of the experiment. The results of the broadening are listed in Table 1.

For comparison we also measured the 15d-f shift due to known electric fields. These are not very accurate measurements because the plates are designed to collect ions and are not large enough to provide a very uniform field. The result is a shift of the $15d_{3/2}$-$15f_{5/2}$ interval of $-10.1$ MHz/(V/cm)$^2$. This is in reasonable agreement with the calculations of the shift of the $15f_{5/2}$ state, which were based on hydrogenic wavefunctions[4] and give $-13.5$, $-12.7$, $-10.0$ and $-6.5$ MHz/(V/cm)$^2$ for the $|m|$=0,1,2 and 3 $\Delta|m| = 0$ transitions. The results of both the measurements and the calculations are given in Figure 5.

As stated earlier, one of the interesting aspects of the presence of ions is that the transition probability for the d-g transition now is of the same order of magnitude as the d-f transition. Hence the shift and the broadening can be measured as described before. Figure 6 shows a one-photon microwave resonance measurement between the $16d_{3/2}$ and $16g_{7/2}$ state. A difference compared to the d-f transition is that the width and the shift is now not only a function of the ion density, but also of the microwave power. This is demonstrated in Figure 7, where the intensity of the d-g transition is plotted for microwave field strengths of 45 and 80 times the field strength used for the d-f resonance measurements. On the basis of power broadening measurements, the latter is estimated as 2 mV/cm.

## 2. Ramsey fringes

A powerful experimental technique for observing the coherence of two atomic states, and therefore also the loss of coherence due to some disturbance, is Ramsey's method of separated oscillatory fields.[5] Let us consider the 17d-f microwave transition. A short microwave pulse is applied. On resonance, after this pulse the actual state is a coherent superposition of the final f state and the initial d state. Both are completely described by a pure wavefunction, each with its own time evolution. The phase difference between the two states grows as $(E_f-E_d)t/h$. At time T later another microwave pulse of duration t is applied to drive the superposition state to the final f state. As the microwave frequency is swept through the resonance, an overall envelope of width 1/t is observed, and the Ramsey interference pattern with spacing 1/T is superimposed on it. The visibility of the interference pattern requires that the phase relation of the d and f state be maintained during the time T between the two microwave

pulses. Thus, collisional dephasing may be readily measured in this way even if the state of the ion is not altered. To realize the short excitation pulses, we placed a fast microwave switch to produce 100-ns pulses between the microwave source and the Na cell. All the other experiments that are reported here are done with continuous microwave power. It is clear that the coherence of the d and f states is partially destroyed by the presence of the ions during the time between the two pulses. We can see this in Figure 8, where a few sets of interference patterns are given; in each case one measured with and one without the presence of ions. It is evident that the interference is less if there are ions present. It is also clear that the envelope of the resonance is not less. Thus the absence of interference is not due to transitions to the other atomic states, but to dephasing. In addition, note that just as in the ordinary resonance measurements, a shift of the transition to lower frequency with increasing ion density can be seen.

## IV. Analysis

### 1 A Priori estimates

To provide some feeling for the orders of magnitude in this process, we will give a rough calculation (in atomic units) for the Na d-f system interacting with an ion. Let us assume that the d state is unaffected by the electric field of the ion and that the f state responds quadratically out to a cut-off field at which point the shift becomes linear. Since the quantum defects of the d and f states differ by an order of magnitude, there is always a region of field strength for which this assumption is valid. To give an idea of this field strength, the cut-off value is given by

$$3n^2E_c/2 = \delta_f/n^3 \quad \text{or} \quad E_c = 3\delta_f/2n^5 \quad . \tag{1}$$

This occurs when the energy difference between the f state and the nearest state (a g state) equals the shift due to the linear Stark effect.

Because the influence of the ions is not constant in time, it is easier to calculate the phase shift rather than calculate directly the energy shift. The phase shift for one collision with impact parameter b is

$$\Delta\phi = \Delta W \Delta t \quad . \tag{2}$$

The order of magnitude for the duration of the collision $\Delta t$ is b divided by the ion velocity v. The average electric field strength during the collision time $\Delta t$ is $1/b^2$. So one collision leads to a phase shift of

$$\Delta\phi = 3n^2/2bv \tag{3}$$

at least, as long as variations of b lead to variations in E that stay in the linear region of the Stark effect. For smaller electric fields than the cut-off value, for larger values of b than that with $E_c$ corresponding to $b_{max}$, the collision is so weak that we ignore the phase shift. In a collision experiment the steady stream of $\Delta\phi$'s gives a constant increment of $\phi$ in time. This is

$$d\phi/dt = \int_0^{b_{max}} \Delta\phi n_i v 2\pi b \, db \qquad (4)$$

where $n_i$ is the density of the ions. Hence the time-averaged energy shift of the f state is

$$\Delta W = n_i n^{9/2} \pi (6/\delta_f)^{1/2} \quad . \qquad (5)$$

This means that the 20f sodium atoms surrounded by ions with a density of $10^6/cm^3$ experience a -0.5 MHz shift, decreasing the d-f splitting by that amount. In view of the intrinsic 20d-f splitting (10.8 GHz) and the intrinsic width of this resonance (0.13 MHz), this seems a measurable shift. The accompanying broadening of the transition is caused by the different collisions suffered by different Na atoms and the tensor polarizability of the f state. Both broadening mechanisms have the same dependence on the electric field as the shift for the f state, linear for $E<E_c$ and quadratic for $E>E_c$. In the case of inhomogeneous electric fields varying from zero to a maximum value, the broadening will also have the same magnitude as the shift. The broadening due to the splitting of the m states is generally much smaller than the average shift of the m states. For instance, Figure 5 shows that in

the particular case of the 15f state, the shift is more than an order of magnitude larger than the splitting bewean the $|m|=0$ and 1 state.

For the d-g transition there is an additional effect -- namely, that the d-g transition is now allowed.

The dipole moment is given by

$$\langle d|\mu|g\rangle = \langle d|\mu|f\rangle\langle f|\mu|g\rangle \frac{E_{ion}}{(E_f - E_g)} \quad . \tag{6}$$

Thus the ratio of the d → f and d → g dipole matrix element is given by

$$\frac{\langle d|\mu|g\rangle}{\langle d|\mu|f\rangle} = \langle f|\mu|g\rangle \frac{E_{ion}}{(E_f - E_g)} \tag{7}$$

For this value to be $\sim 10^{-2}$, we require $E_{ion}$ = 80 mV/cm, in the case of a 16 d-g transition.

2. Space charge effect

The ion density required to obtain measurable effects in the above example is evidently much larger than the ion densities actually used in the experiment. Therefore, we consider now the macroscopic effect that the ions have on the Rydberg atoms in addition to their microscopic effect. Specifically the ions are generated along the cylinder of overlap of the orange (Na $3s_{1/2}$-$3p_{1/2}$) and the UV (Na $3p_{1/2}$-continuum) beams. These ions give rise to an electric field E of

$$E = \lambda/2\pi\varepsilon_0 r \tag{8}$$

where $\lambda$ is the linear ion density), at a distance r from the center of the beam, as long as r is larger than the radius of the beam of ions itself, ~ 1 mm. At distances smaller than the radius of the beam, the electric field is linearly increasing with r. Hence the maximum field strength is at the surface of the cylinder of the charge. If we substitute a typical experimentally observed density, we find fields of ~ 0.5 V/cm, which are sufficient to produce the observed results: a shift and a broadening of the 15d-f transition of 14 MHz. Experimentally we observed that roughly 30 dB more microwave power is needed to drive the 16d-g transition with the same intensity as the 16d-f transition. This means a ratio of 30 for the corresponding field strengths. Equation 7 allows us to calculate from this ratio of 30 an absolute field strength due to the ions in the case of a d-g transition of 0.25 V/cm. Again, this experimental value is in reasonable agreement with the estimations based on the space charge.

## V. Conclusion

The experimentally observed shifts and broadenings are much larger than would be expected on the basis of microscopic ion-atom collisions. Rather, the observed results are due to the generally ignored macroscopic space charge fields of the ions. Thus, these experiments point out the importance of even very small numbers of ions in any application involving Rydberg atoms.

Finally, although the effects we report are due to macroscopic space charge, which may not be widely applicable, the results do indicate that ions may be more generally used to collisionally induce dipole moments by their long range coulomb interaction. This work was supported by the Air Force Weapons Laboratory.

## REFERENCES


1. D. Rogovin and P. Avizonis, Appl. Phys. Lett. 38 ,666 (1981).
2. D. Rogovin, P. Avizonis and J. Filcoff, Opt. Lett. 8, 268 (1983).
3. T. F. Gallagher, R. M. Hill and S. A. Edelstein, Phys. Rev. A 13, 1448 (1976).
4. H. A. Bethe and E. A. Salpeter, Quantum Mechanics of One and Two Electron Atoms (Academic, New York,1957).
5. N. F. Ramsey, Molecular Beams (Oxford University, London, 1956).

TABLE 1. Shift and broadening of the $nd_{3/2}-f_{5/2}$ and $16d_{3/2}-g_{7/2}$ transitions due to ions.

| State | Shift $\Delta$(Hz/(ions/cm$^3$)$^2$) | Broadening $\Gamma$(Hz/(ions/cm$^3$)$^2$) |
|---|---|---|
| $15d_{3/2}-f_{5/2}$ | $-2.5 \cdot 10^{-4}$ | $5.6 \cdot 10^{-4}$ |
| $16d_{3/2}-f_{5/2}$ | $-5.3 \cdot 10^{-4}$ | $8.3 \cdot 10^{-4}$ |
| $17d_{3/2}-f_{5/2}$ | $-1.2 \cdot 10^{-3}$ | $2.9 \cdot 10^{-3}$ |
| $16d_{3/2}-g_{7/2}$ + | $-2.5 \cdot 10^{-4}$ | $7.2 \cdot 10^{-4}$ |
| $16d_{3/2}-g_{7/2}$ * | $-3.2 \cdot 10^{-4}$ | $1.5 \cdot 10^{-3}$ |

+$E_{mw}$ = 90 mV/cm

*$E_{mw}$ = 160 mV/cm

## FIGURE CAPTIONS

FIGURE 1. Relevant levels for the observations of the d-f and the d-g resonances of the n = 16 state of sodium. The straight arrows indicate the two laser pumping steps. The wavy arrows down indicate the most probable fluorescent decay of the 16g and 16f state. Finally the curved arrows indicate a one-photon microwave transition. In all cases only the state with the lowest j-value of the doublet is observed.

FIGURE 2. Frequency scans in the vicinity of the $16d_{3/2}$-$16f_{5/2}$ resonance for different ion densities. For reference, curve a is given, which is measured without ions in the cell. For the curves b, c, and d, the ion density is 3, 5 and 9 x $10^5$ ions/$cm^3$, respectively.

FIGURE 3. Shift of several resonance lines as a function of the square of the ion density. The scattering of the data is due mainly to uncertainties in the cell temperature, which influences both the ion and the atom density. ◇ $17d_{3/2}$-$f_{5/2}$, □ $d_{3/2}$-$f_{5/2}$, ○ $15d_{3/2}$-$f_{5/2}$, ▽ $16d_{3/2}$-$g_{7/2}$ at 90 mV/cm microwave field, □ $16d_{3/2}$-$g_{7/2}$ at 160 mV/cm microwave field.

FIGURE 4. Width of several resonance lines as a function of the square of the ion density. Legend as in Figure 3.

FIGURE 5. Measurements and calculations of the shift of the $15d_{3/2}$-$f_{5/2}$ transition due to a constant electric field. The measurements consist only of $|m| = 0$ and 1.

FIGURE 6. Frequency scans around the $16d_{3/2}$-$g_{7/2}$ resonance for different ion densities. The ion densities are 3, 5 and $9 \times 10^5$ ions/cm$^3$ for curve a, b, and c. In all three cases the microwave field strength is 160 mV/cm.

FIGURE 7. Intensity of the $16d_{3/2}$-$g_{7/2}$ resonance as a function of the ion density for two different field strengths of the microwave field. The ratio of the field strengths is rather accurately known as 1.78. The absolute values of 90 and 160 mV/cm are less accurate. The two most left data points indicate lower limits.

FIGURE 8. Ramsey interference pattern for the $17d_{3/2}$ - $17f_{5/2}$ transition. The time difference between the first and the second microwave pulse is 0.3, 0.4, 0.5 and 0.7 μs for Figures a,b,c and d, respectively. Note that loss of interference is increasing with increasing time difference between the excitation pulses.

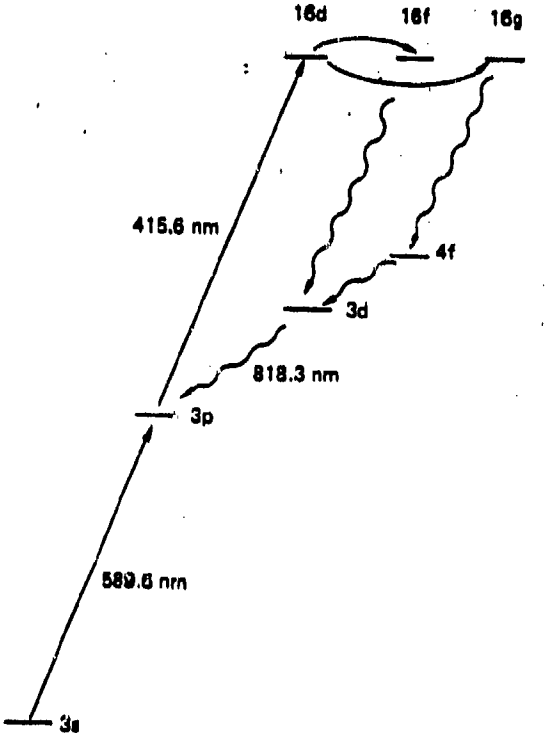


FIGURE 1

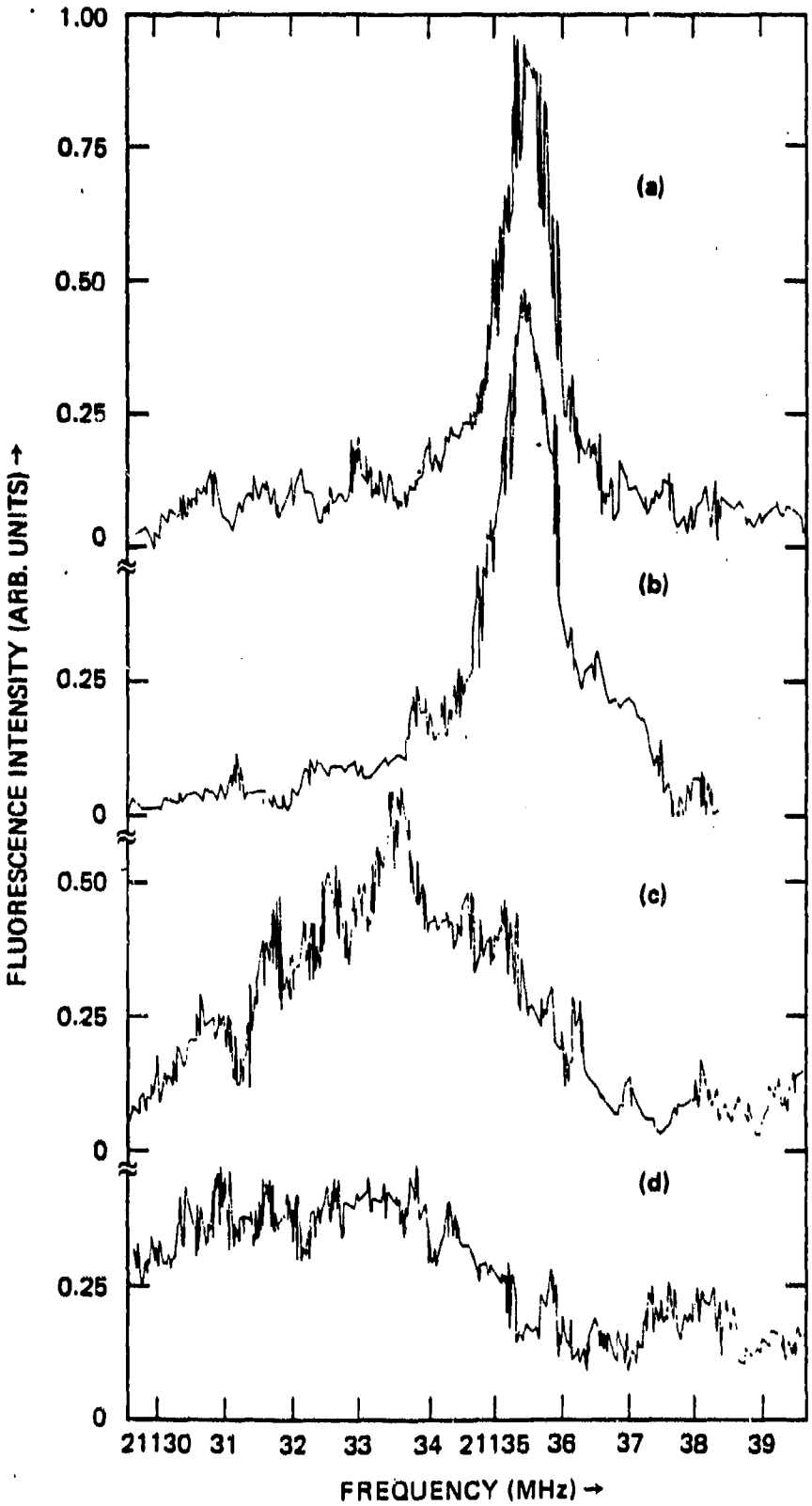
1.00
0.75
0.50
0.25
0
(a)
(b)
(c)
(d)
FLUORESCENCE INTENSITY (ARB. UNITS) →
21130 31 32 33 34 21135 36 37 38 39
FREQUENCY (MHz) →

FIGURE 2

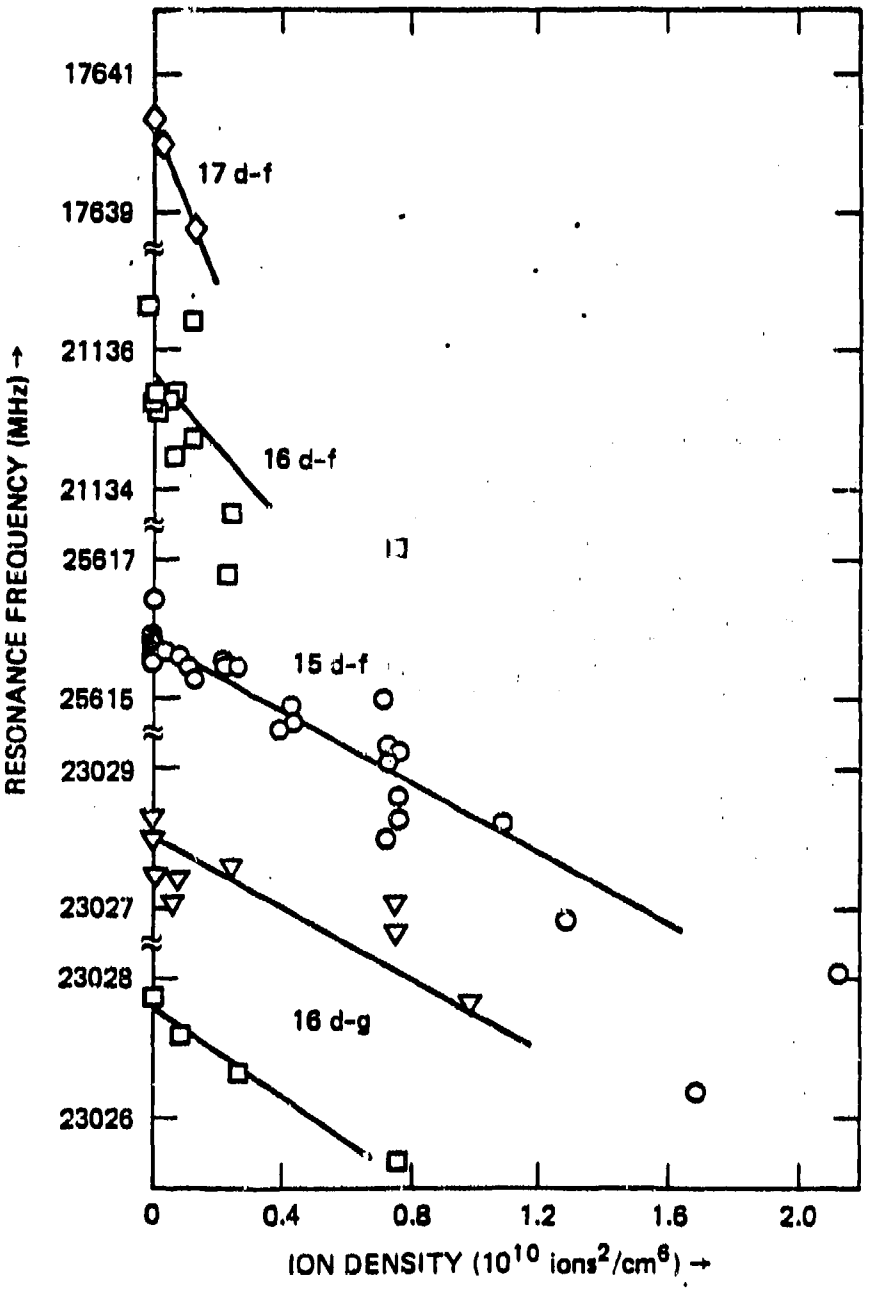
17641
17639
21136
21134
25617
25615
23029
23027
23028
23026
17 d-f
16 d-f
15 d-f
16 d-g
RESONANCE FREQUENCY (MHz) →
0
0.4
0.8
1.2
1.6
2.0
ION DENSITY ($10^{10}$ ions$^2$/cm$^6$) →

FIGURE 3

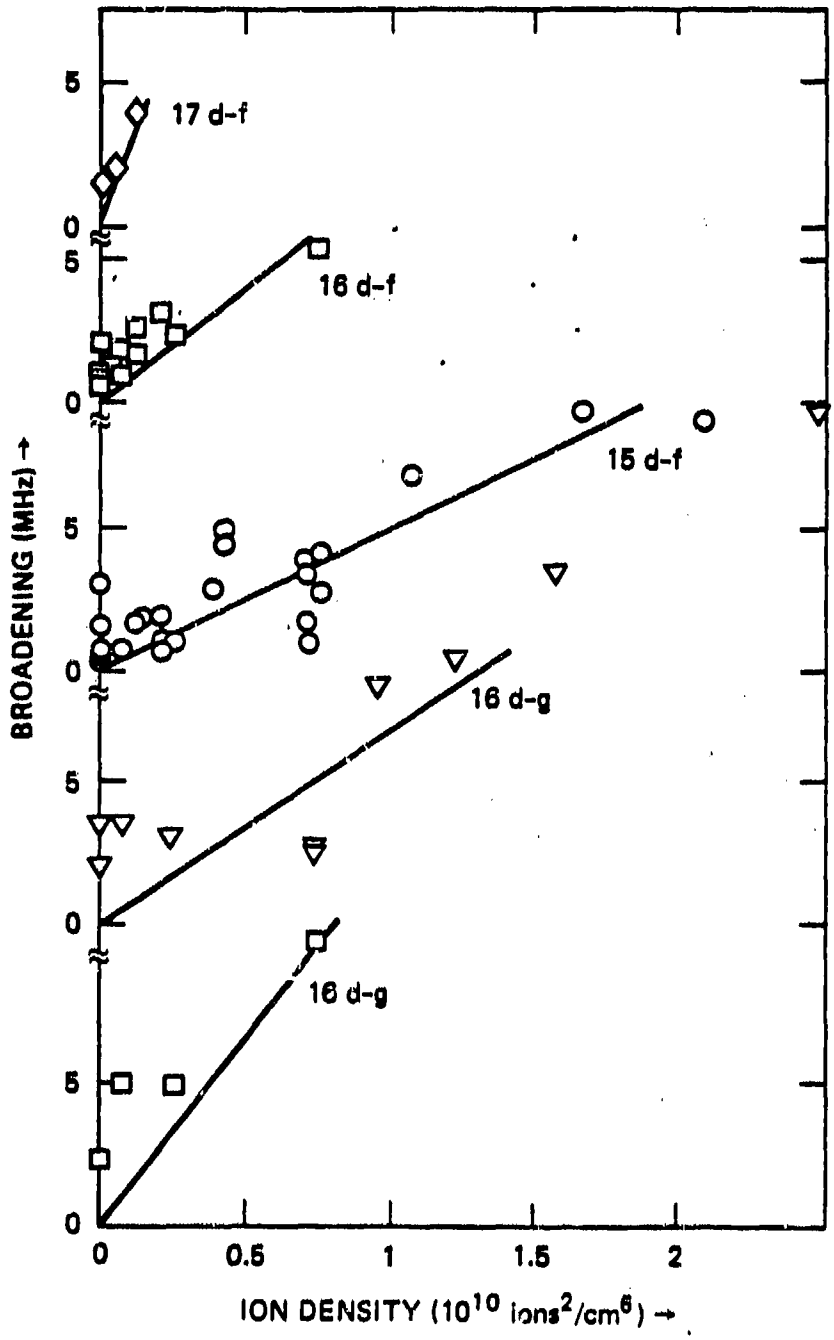
17 d-f
16 d-f
15 d-f
16 d-g
16 d-g
BROADENING (MHz) →
ION DENSITY ($10^{10}$ ions$^2$/cm$^6$) →
0
0.5
1
1.5
2

FIGURE 4

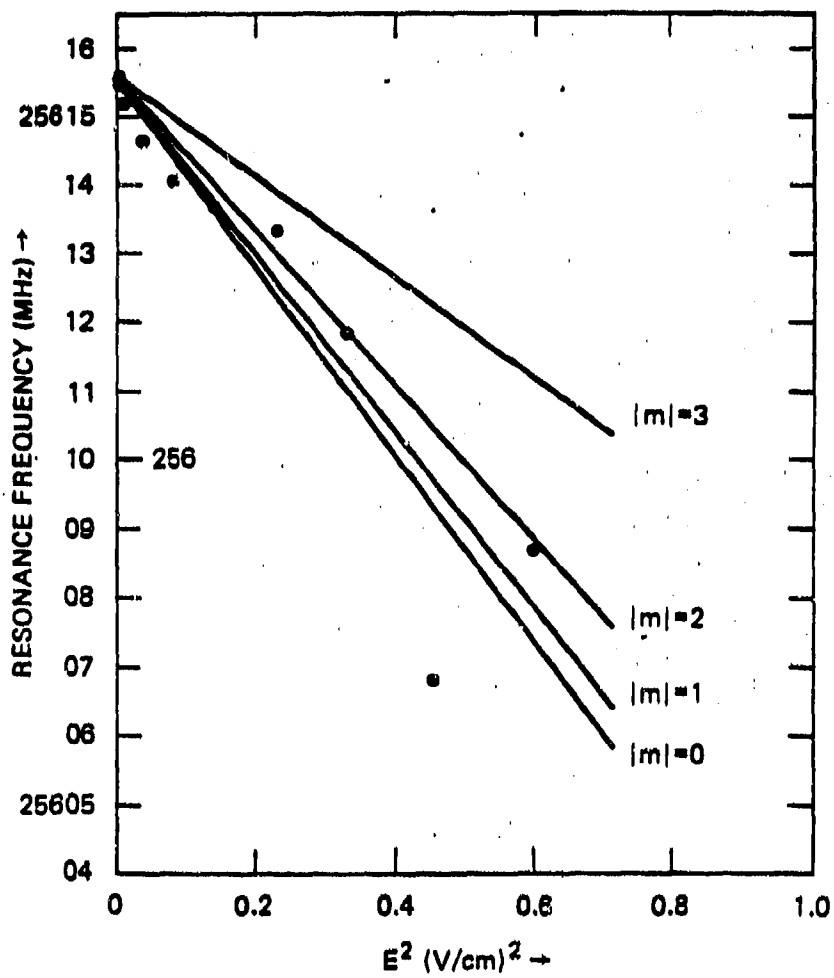
16
25615
14
13
12
11
10
09
08
07
06
25605
04
256
RESONANCE FREQUENCY (MHz) →
0
0.2
0.4
0.6
0.8
1.0
E² (V/cm)² →
|m|=3
|m|=2
|m|=1
|m|=0

FIGURE 5

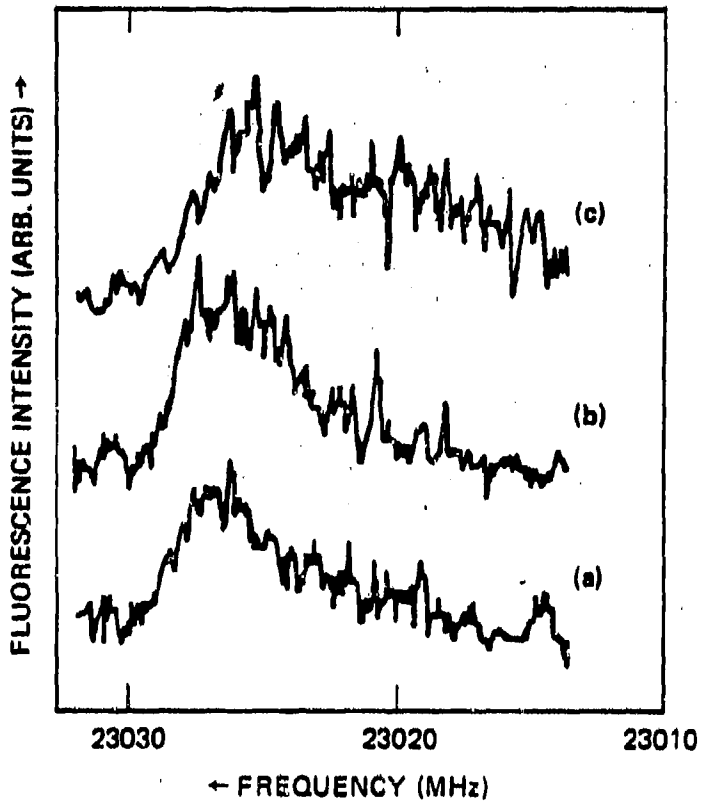
FLUORESCENCE INTENSITY (ARB. UNITS) →
(c)
(b)
(a)
23030
23020
23010
← FREQUENCY (MHz)

FIGURE 6

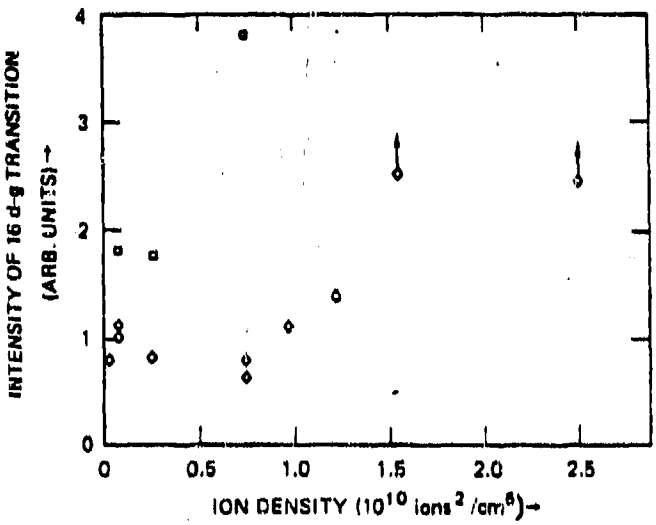
INTENSITY OF 16 d-g TRANSITION
(ARB. UNITS) →
4
3
2
1
0
0
0.5
1.0
1.5
2.0
2.5
ION DENSITY ($10^{10}$ ions$^2$ /cm$^6$)→

FIGURE 7

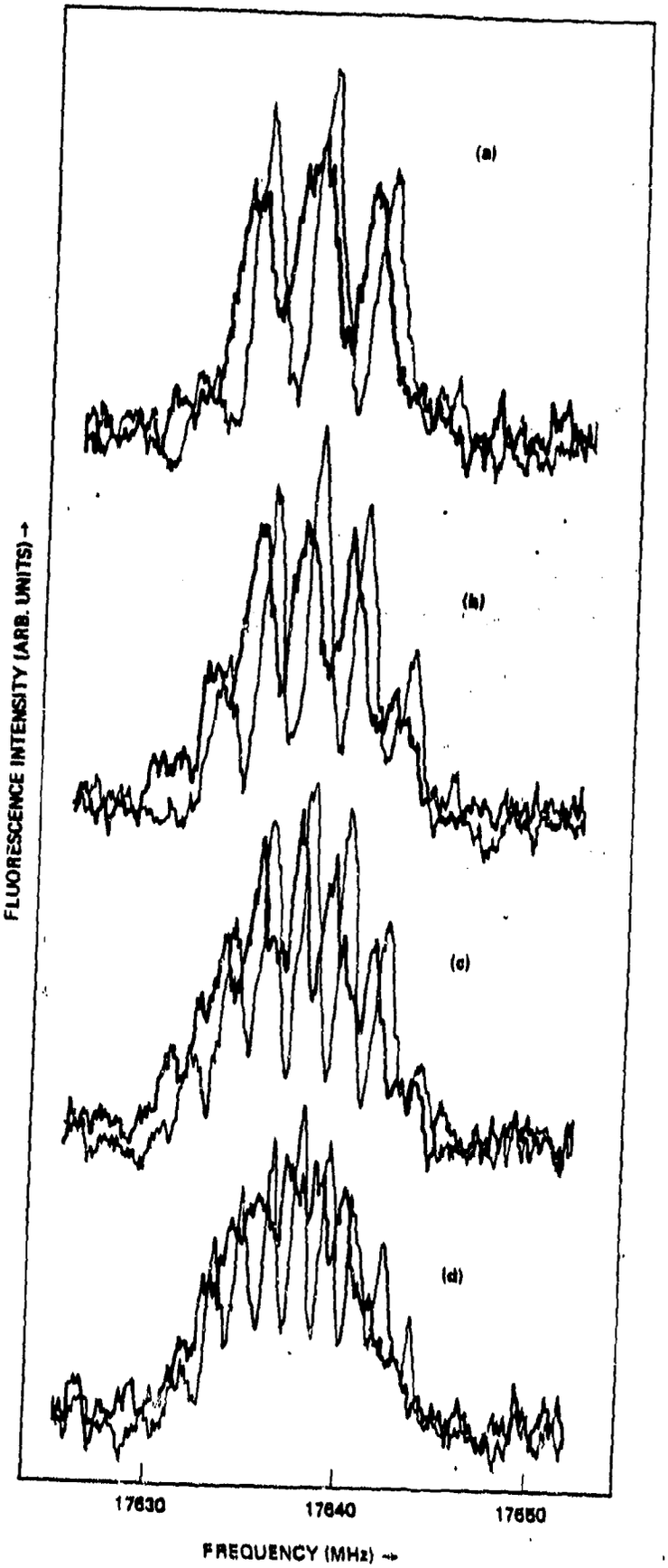
(a)
(b)
(c)
(d)
FLUORESCENCE INTENSITY (ARB. UNITS) →
17630
17640
17650
FREQUENCY (MHz) →

FIGURE 8